LAL 90-87
December 1990

Laboratoire de l'Accélérateur Linéaire

RECENT PHYSICS RESULTS FROM LEP

J.-E. Augustin

Invited talk at the ICFA Seminar, Protvino, October 1990

U.E.R
de
l'Université Paris-Sud

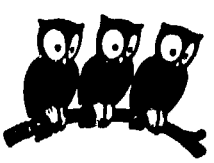

Institut National
de Physique Nucléaire
et
de Physique des Particules

Bâtiment 200 - 91405 ORSAY Cedex

LAL 90-87
December 1990

RECENT PHYSICS RESULTS FROM LEP

J.–E. Augustin

Laboratoire de l'Accélérateur Linéaire, IN2P3–CNRS
et Université de Paris–Sud, F–91405 Orsay Cedex, France

The Large Electron Positron (LEP) collider built at CERN began operation in August 1989, when the first multihadronic events from Z^0 decay were detected. Already very significant results were achieved by the end of that year, but the statistics gathered in 1990 is seven times larger, and allows already very detailed physics studies. This very fast startup of a gigantic new machine was matched by the rapid commissionning of the four large detectors set-up to observe the collision products: Aleph, Delphi, L3, and Opal. After mentionning the machine operations, the recent observation of transverse beam polarization, and the luminosity measurements, I shall review the most important results obtained up to now on the tests of the electroweak sector of the Standard Model. This includes the Z^0 excitation curve parameters in hadronic and leptonic modes, the forward-backward asymmetries of the leptons, the detection of the polarization of the taus, and the corresponding results on the number of light neutrinos, on the electroweak coupling constants and mixing angle, and on the top quark mass. Some hadronic physics results and QCD studies will be reported before summarizing the results for particle searches, notably the Higgs boson. The choices made are quite arbitrary, and cannot do justice to the impressive amount of progress made in these few months, as attested by the some sixty papers already published by the four collaborations. In this talk, I will rely heavily on these publications, and especially on the review[1] prepared by F.Dydak for the Rochester Conference held this summer in Singapore.

*invited talk at the ICFA seminar, Protvino, October 1990

Machine Operation

After one year of operation, most the LEP accelerator parameters achieved are above the design values of the project. This is the case for the stored and accelerated currents in the beams, their emittences in both directions, and the crossing point betatron amplitude functions. A notable difference was observed for the vertical beam-beam tune shift parameter, which was limited at about .02, half the expected .04, so that the maximum luminosity reached is still about twice lower than the design 1.7 $10^{31}cm^{-2}sec^{-1}$. The reasons for this are not all understood.

One important observation is that the luminosity delivered to each of the four interaction points was consistently at variance, the difference beeing 20% between the extremes. This is reflected, together with the data taking efficiencies, in the statistics recorded by each experiment (Table 1). This early

	Z^0 hadronics	$\int \mathcal{L}\, dt$ (pb^{-1})
Aleph	170K	9.7
Delphi	120K	8.0
L3	120K	7.8
Opal	150K	9.0
$\sum$	560K	
with Leptons	620K	

Table 1: LEP running in 1990

appearence of the beam-beam effect is the subject of vigorous studies, and the guidance of simulation programs is of great help. Many improvements were obtained during the running period, and at the end of August, a record 1.5 pb^{-1} could be delivered in a week.

Transverse Polarization

One important development has been the observation of transverse polarization in the LEP beams [2]. This polarization occurs through the well known Sokolov-Ternov mechanism of spin dependent radiation in the orbit magnetic field, and is detected through the Compton backscattering of

a circularly polarized laser beam: the centroid of the scattered photons is vertically displaced proportionnally to the beam polarization.

After very detailed tests of the polarimeter system, and having in hand all necessary checking procedures, the LEP ring was specially tuned to an energy point where depolarizing effects were expected to be minimum. The figure 1 shows the time evolution of these measurements. All effects observed are statistically consistent with a polarization of $(9 \pm 3)\%$, of the order of the expectation. This observation will be used to calibrate the beam energy through resonant depolarization, to an accuracy better than $5\ 10^{-5}$.

This will already be an important contribution to physics, since it will improve the accuracy on the Z^0 mass by a factor larger than 4. But the ultimate aim of these studies is to find the conditions where 50% longitudinally polarized beams can be kept in collisions: this would allow an entirely new set of Standard Model studies [3]. There is still a long way to go before this is reached, and this first result is very stimulating.

Luminosity Measurement

One of the important experimental breakthroughs at LEP has been the unprecedented accuracy reached in the measurement of the normalizing process, the so-called luminosity measurement. This is done by detecting electron-positron quasi-elastic scattering at small angles, typically from 40 to 100 mrad. In that case, the rate is entirely dominated by the QED t-channel photon exchange process, and is independent from the Z^0 parameters. The detection must allow in a controlled way for the presence of an additional photon and the cross-section is theoretically computed [4] including this radiation effect.

One of the main difficulties of this measurement is the very fast angular decrease of the rate with the scattering angle, so that the minimum detection angle must be known with high precision. The four LEP experiments have made good use of the previous experience from lower energy colliders, and their small angle detectors include excellent electromagnetic calorimeters, precise tracking, and sophisticated trigger and background monitoring systems [5] [6] [7] [8]. The accuracy in the detection angle is obtained by the measurement of the position of the electron showers to a few tenth of a millimeter, except in Delphi where a precisely machined lead mask is used.

Very detailed simulations of the detectors have been performed, and the understanding of every aspect of the data has allowed to put stringent limits on unknown systematic sources of error, reaching less than one percent.

This accuracy is very useful for the precision on the Z^0 excitation curve *measurements*, but its use is now limited by the uncertainty on the theoretical calculation of the cross-section, which is estimated to be 0.7 to 1%. So that LEP asks for higher order QED computations, similarly to the *g-2* experiments: LEP is metrology at high energy.

1 Electro-Weak Model Studies

1.1 Z^0 Excitation Curve

The excitation of the Z^0 resonance is by far the dominant feature of the total electron-positron annihilation cross-section around an energy of 90 GeV in the center-of-mass system. At the top of the curve, the inelastic unitarity limit in P-wave is reached: $\sigma_0 = 3\pi\lambda\!\!\!^{-2} B_{e^+e^-}$ where $\lambda\!\!\!^{-} = 2/M_Z$ is the deBroglie wavelength of the electron, and $B_{e^+e^-} = \Gamma_{e^+e^-}/\Gamma_Z$ is the branching fraction of Z^0 into e^+e^- . This amounts to about 60 nb, or a value of almost 6000 for the ratio R to the $\mu^+\mu^-$ electromagnetic cross-section. The energy dependance around M_Z is the ususal Breit-Wigner curve, and the bare cross-section to a particular final state *f* is:

$$\sigma_0^f(s) \simeq \frac{12\pi\Gamma_{e^+e^-}\Gamma_f}{M_Z{}^2} \frac{s}{|s - M_Z{}^2 + iM_Z\Gamma_Z|^2} \qquad (1)$$

In the Standard Model of electroweak interactions, the Z^0 is coupled to all kinematically accessible fermion-antifermion pairs *f* with couplings depending on the SU(2) and U(1) invariance properties of the fermion. The vector and axial Z^0 couplings g_V^f and g_A^f depend upon the 3rd component of weak isospin I_3^f and on the charge Q_f of the fermion according to $g_A^f = I_3^f$ and $g_V^f = I_3^f - 2\sin^2\theta_W Q_f$, where θ_W is the weak mixing angle with $\sin^2\theta_W = 1 - M_W{}^2/M_Z{}^2$.

The formula 1 is exact for a $\nu\bar{\nu}$ final state. For charged fermions. one has to add the photon annihilation amplitude which contributes to the cross-section through its square at the top, and also through its interference with

the Z^0 term on the sides. The matrix element is thus:

$$\frac{Q_e Q_f 4\pi\alpha}{s} J_\mu^e J^{\mu f} + \frac{\sqrt{2}\rho G_F {M_Z}^2}{s - {M_Z}^2 + i M_Z \Gamma_Z} Z_\mu^e Z^{\mu f} \qquad (2)$$

with J_μ the electromagnetic current $\bar{v}\gamma_\mu u$, and Z_μ the neutral weak current $\bar{v}\gamma_\mu(g_V^f - \gamma_5 g_A^f)u$. G_F is the muon decay constant. ρ is equal to 1 if there are only Higgs doublets to break the SU(2) symmetry, as in the minimum version of the Standard Model, or in its Minimum Supersymmetric extension (MSSM). It is given in general by $\rho = {M_W}^2/({M_Z}^2 \cos^2\theta_W)$.

In the special case of e^+e^- final states, the t-channel exchange diagrams have also to be taken into account.

But the cross-section reachable experimentally is somewhat different from this computation. It has to take into account the effects of the higher order terms. The most spectacular one is the energy smearing from the real photon emission accompanying the basic process. It can be understood as a bremsstrahlung of the initial electron and positron prior to the annihilation: the energy available is thus reduced, and one observes a convolution of the bare cross-section with this available energy distribution. In most cases, the radiated photons go undected in the beam pipe together with the outgoing beam, so that the correction is quite detector independent. It is shown on figure 2 in the case of the $\mu^+\mu^-$ [9]. The top cross-section is reduced by about 25%, the maximum is displaced from the Z^0 mass, and the width is increased by the shape distorsion. These large effects have been computed to an excellent accuracy. The computation must take into account the interference with the final state radiation, and the inclusion of higher order terms.

The virtual electro-weak radiative corrections have also to be taken into account for a proper evaluation of the predictions of the theory: one way to do this is to use renormalized values of the coupling constants evaluated at the Z^0 mass. One can then write the expression of the Z^0 excitation curve using an expression similar to formula 2, but using effective parameters[10]. In the present case, one has to use an improved propagator with imaginary part $i(s/{M_Z}^2)M_Z\Gamma_Z$, a value of α corrected for vacuum polarization up to $s = {M_Z}^2$, Z^0 couplings with an effective $\sin^2\overline{\theta_W} = \sin^2\theta_W - \cos^2\theta_W(\bar{\rho} - 1)$, and

$$\bar{\rho} = 1 + \frac{3G_F {m_t}^2}{8\sqrt{2}\pi^2} \qquad (3)$$

This last correction comes from the lack of cancellation between the weak isospin doublet members top and b quarks, due to their large mass difference. It is what allows LEP to give limits on the top mass m_t .

The aim of the measurements is to extract from the observed cross-sections in the different final states, various sets of parameters to be compared with these predictions. Up to now the channels explored are the sum of all quark-antiquark channels in the hadronic final states, and the three leptonic channels separately. For example, figure 3 shows the results from Opal [11], with the line shape fits superimposed. A fit to the very precise hadronic cross-section allows first a determination of the mass of the Z^0 , and a measurement of the its total width Γ_Z together with the hadronic partial width Γ_h or with the hadronic peak cross-section.

	M_Z (GeV/c^2)	Γ_Z (GeV/c^2)	Γ_h (MeV/c^2)
Aleph	91.186±0.013	2.506±0.026	1764± 23
Delphi	91.188±0.013	2.476±0.026	1756± 31
L3	91.161±0.013	2.492±0.025	1748± 35
Opal	91.174±0.006	2.505±0.020	1778± 24
Average	91.177±0.031	2.496±0.016	1764± 16
χ^2/dof	0.93	0.32	0.20

Table 2: Results on M_Z , Γ_Z and Γ_h .

The results of the experiments are shown in table 2[1]. There is a good agreement between the experiments. A common systematic error is included in the averages. For the Z^0 mass, it comes from the LEP energy calibration, which is now about 30 MeV, dominating over the 6 MeV statistical precision. This should be greatly improved soon using calibration from resonant depolarization, which is expected to reduce this systematic uncertainty to less than 5 MeV. The Z^0 mass allows to compute Standard Model predictions for the other results. The prediction for the hadronic peak cross section σ_0^h is almost independent from the top quark mass, and therefore provides for a clean test of the predictions. It is computed to be 41.30 ± 0.10 nb, when the average measurement is 41.78 ± 0.52 nb. The agreement is excellent.

The excitation curves of the lepton final states are still less precise due to the much lower statistics. Figure 4 shows the results[12] from L3. The

various contributions to the e^+e^- final state are well shown. The unfolding of the t-channel exchange contribution introduces a systematic uncertainty particular to this channel. Nevertheless, they already allow other precise tests of the model. The averages of the LEP experiments are compared to the Standard Model value in Table 3, and the agreement is again found excellent.

	LEP Average (MeV/c^2)	Standard Model
$\Gamma_{e^+e^-}$	83.6±1.0	83.8±0.9
$\Gamma_{\mu^+\mu^-}$	84.1±1.4	
$\Gamma_{\tau^+\tau^-}$	83.2±1.5	
$\Gamma_{l^+l^-}$ (Universality)	83.7±0.7	83.8±0.9
Γ_{inv}	482±16	502±5

Table 3: Results on Z^0 Leptonic and invisible Widths

Most importantly, the measurement of the leptonic partial width of the Z^0 gives the best estimate of the number of massless neutrinos. For this, one first estimates the invisible witdh defined as Γ_Z -Γ_h -$3\Gamma_{l^+l^-}$, that is everything which was not included in the hadrons or charged leptons. The LEP result is also shown in table 3. The number of neutrinos is obtained in dividing this invisible width by the $\nu\bar{\nu}$ width. In practice, the best model independent measure is obtained through the formula 4:

$$N_\nu = \frac{\Gamma_{inv}}{\Gamma_{\nu\bar{\nu}}} = \frac{\Gamma_{l^+l^-}}{\Gamma_{\nu\bar{\nu}}}\left[\sqrt{\frac{12\pi\Gamma_h/\Gamma_{l^+l^-}}{\sigma_0^h M_Z{}^2}} - \frac{\Gamma_h}{\Gamma_{l^+l^-}} - 3\right] \qquad (4)$$

so that the experimental values for the top hadronic cross section σ_0^h and the ratio of the hadronic to the leptonic width are used together with the Z^0 mass. The only theoretical input is the ratio of the leptonic to the neutrino widths, computed to be 0.5010 ± 0.0005. The resulting value from the average[1] of the four LEP experiments is

$$N_\nu = 2.89 \pm 0.10$$

very near to 3. This is a definite proof that there does not exists other families having standard neutrinos with a mass less than about 40 GeV/c^2 . This is most dramatically seen on the hadronic excitation curves, as in figure 5 from Delphi[13].

1.2 Forward-Backward Asymmetries

The study of the angular distribution of the fermion pair produced in the Z^0 decay gives access to independent measurements of the vector and axial couplings g_V^f and g_A^f . The interference between the axial and vector amplitudes gives rise to a forward-backward asymmetry in the angular distribution of the fermion. If one defines θ as the polar angle between the fermion and the electron,

$$A_f^{FB} = \frac{\{\int_0^1 \frac{d\sigma}{d\cos\theta} d\cos\theta - \int_{-1}^0 \frac{d\sigma}{d\cos\theta} d\cos\theta\}}{\{\int_0^1 \frac{d\sigma}{d\cos\theta} d\cos\theta + \int_{-1}^0 \frac{d\sigma}{d\cos\theta} d\cos\theta\}}$$

where $\frac{d\sigma}{d\cos\theta}$ is the differential cross-section w.r.t. θ. At the top of the Z^0 , this asymmetry is expected to be:

$$A_f^{FB}(M_Z{}^2) = \frac{3}{4}\mathcal{A}_e\mathcal{A}_f = \frac{3}{4}\frac{g_V^e g_A^e}{(g_V^e{}^2 + g_A^e{}^2)}\frac{g_V^f g_A^f}{(g_V^f{}^2 + g_A^f{}^2)}$$

and a measurement of this asymmetry together with the corresponding partial width will give directly the couplings, in fact the square of the leptonic coupling if one assumes universality to hold. Here again, a precise knowledge of the radiative corrections is necessary, and the computations have been done [14]. The figure 6 shows the asymmetries as measured by the Aleph experiment [15]. The energy dependance of the asymmetries is dominated by the absorptive part of the propagator, and varies strongly across the resonance. From the common fit to these asymmetries and to the excitation

	LEP Average
g_V^l	-0.045±0.006
g_A^l	-0.501±0.002

Table 4: Results on leptonic neutral current couplings

curves, one gets the values for the leptonic couplings shown in table 4, where the signs are taken from neutrino scattering experiments .

The axial value is in excellent agreement with the value of $\frac{1}{2}$. The vector one is consistent with $\sin^2\overline{\theta_W}$ below $\frac{1}{4}$ as measured at lower energies.

1.3 Tau Polarization

At the heart of the Standard Model is its very peculiar spin structure. It would best be studied with longitudinally polarized beams, but it can readily be accessed with the analysing power provided by the parity violating $\tau^+\tau^-$ decays. The polarization of the τ 's in the final state, also called the polarization asymmetry is given by:

$$P_\tau = A^\tau_{pol} = -2\mathcal{A}_\tau = -\frac{2g^\tau_V g^\tau_A}{g^{\tau\,2}_V + g^{\tau\,2}_A}$$

As known since long, the τ polarization in Z^0 decays can be measured through the momentum distribution of the electron or muon[16] in the tau beta decay, and most directly of the pion spectrum [17] of the $\tau \rightarrow \pi\nu_\tau$ decay which is fully polarized. Moreover, the τ is a member of the high mass family, and its detailed properties should be especially looked at.

The present statistics are still poor for these studies. Preliminary results are shown on figure 7 for the muon momentum spectrum[18], and on figure 8 for the pion spectrum[19]. The expected effects are present, but still with large statistical uncertainties. From its own set of measures, Aleph gives[19]

$$P_\tau = -0.157 \pm 0.055$$

from which one can compute independently $\sin^2\overline{\theta_W} = 0.231 \pm 0.007$, already a significant result, in excellent agreement with other values.

1.4 Standard Model Parameters

Many other studies of the electro-weak sector have been done, in particular preliminary measurements of the partial widths and asymmetries into heavy quarks, but the precision is still low. From this whole set of results, and assuming all other parameters as predicted by the Standard Model, one can extract the values of the effective weak mixing angle $\sin^2\overline{\theta_W}$ shown in table 5. This observed value of $\sin^2\theta_W(M_Z{}^2)$ is independent of any correction from the top quark mass m_t .

Conversely, the LEP results on M_Z and $\sin^2\overline{\theta_W}$ can be combined with the measurement of M_W /M_Z at $p\bar{p}$ colliders[20], to get an estimate of this top

Aleph	0.2288±0.0023
Delphi	0.2309±0.0047
L3	0.2272±0.00033
Opal	0.2315±0.0024
Average	0.2296±0.0020
χ^2/dof	0.43

Table 5: $\sin^2\overline{\theta_W}$ from LEP Results

quark mass. The identification of the Fermi theory with the effective Standard Model at low energy, and the use of the improved Born approximation of section 1.1, gives the relation:

$$M_Z{}^2 = \frac{\pi\alpha(M_Z{}^2)}{\sqrt{2}G_F\bar{\rho}\sin^2\overline{\theta_W}(1-\sin^2\overline{\theta_W})}$$

where $\alpha(M_Z{}^2) = (128.79\pm0.12)^{-1}$. Using M_Z and $\sin^2\overline{\theta_W}$ as measured above, one get a value of $\bar{\rho}$, and thus m_t from equation 3. The result is:

$$m_t = 137 \pm 40 \text{ GeV/c}^2$$

A detailed analysis has been published by Ellis and Fogli [21], who get, including also neutrino scattering results and low energy data:

$$m_t = 127^{+24}_{-30} \text{ GeV/c}^2$$

which is already significantly less than 200 GeV/c^2 . Once the top mass will be experimentally known, the next correction to ρ, which depends logarithmically on M_H , could give access to limits in the Higgs mass.

2 Hadronic Results and QCD Studies

The large statistics of $q\bar{q}$ events detected at the Z^0 energy allow specific studies of the the fragmentation into hadrons, and also of the QCD gluon radiation in multijet events. The study of the events shape variables and their comparison to the available Monte Carlos has first been done to check the understanding of the detectors and control the detection efficiencies to

multihadrons. For this study, event shape variables are compared to the Monte Carlo generated counterpart. A detailed simulation takes care of the small distorsions due to the detector. The generator parameters are then tuned if necessary to fit the data. The figure 9 shows as an example the results observed by the Opal experiment[22] on the sphericity and aplanarity distributions compared to various Monte Carlos ; the lower insert shows the difference between data and fits in units of standard deviations: the agreement is excellent.

The next step is thus to use specific properties of the $q\bar{q}$ events to try and study QCD itself. Quite detailed studies have already been made, but I will report here only on the determination of the QCD coupling constant α_s.

The most simple way is to fit the multijet distribution with the QCD predicted gluon radiation. This turns out to be quite complicated in practice, due to the arbitrariness in defining jets, as well as in assuming identity between jets and partons. Nevertheless, the detailed studies at Petra and PEP energies have led to a procedure which has been proven to minimize these drawbacks. In an event, the particles are clusterized in jets using the JADE algorithm: any particle is paired with the neighbour such that the quantity

$$y_{ij} = \frac{m_{ij}^2}{E_{vis}^2}$$

is smallest. m_{ij} is the invariant mass of the pair, and E_{vis} the event visible energy. The pair is merged in a pseudo-particle with the sum of the momenta, and the process is iterated until a certain value y_{cut} is reached: the remaining pseudo-particles are the jets. Second order (α_s^2) QCD predicts rates of up to 4 partons. A similar process is applied to these QCD events by merging the partons up to a value y. It has been checked [23] that the y and y_{cut} values at which partons and jets switch from 3 to 2 jets are statistically identical. A comparison of the theoretical and experimental multijet rates, as shown on figure 10 from L3[24] yields then a direct measurement of α_s. One drawback of this method is the undetermination of the QCD scale μ^2 of the process, and its variation enters as a systematic uncertainty.

Various more sophisticated methods are studied to minimize the effects of hadronization. The energy-energy correlations are defined as an energy weighted histogram of all angles between pairs of particles. The left-right

difference of this histogram defines the asymmetry in energy-energy correlation. It is insensitive to the fragmentation process which changes the energy-energy correlation symmetrically. The Delphi experiment [25] has studied this difference histogram (figure 11). A fit to the QCD prediction yields an independent determination of α_s. The mean value determined at LEP is:

$$\alpha_s(M_Z{}^2) = 0.116 \pm 0.012$$

where the systematic error is dominated by the uncertainty on the renormalization scale. The high statistics available will allow soon to improve on these studies, and give access to finer tests of QCD.

3 New Particle Searches

A considerable amount of work has been invested, since LEP startup, in the search for any unexpected feature in the data. The measurement of the Standard Model parameters can be used to place indirect limits on particles beyond the accessible energy range of LEP, or to feel their effect as we have seen for the top quark. The knowledge of the "invisible" width Γ_{inv} is used to place limits on the presence of unknown decay products of the Z^0 .

Direct searches have been made for signals in particular final state topologies. Up to now, the results are negative, but this should not be taken as the final answer: for most of these studies, higher statistics, and later higher energies with LEP200, will allow more refined searches. The main results are :
No new standard quark of bottom or top type exists below 46 GeV/c^2 ,
No sequential heavy lepton below 44.3 GeV/c^2 ,
No supersymmetric partners of quarks and leptons below 43 to 45 GeV/c^2 , and no neutralinos nor charginos below 45 GeV/c^2 .
A specially important search concerns the Standard Model Higgs particle H^0, whose mass is totally unknown. The production mechanism is :

$$e^+e^- \rightarrow H^0 + Z^{0*} \qquad (5)$$

with the virtual Z^0 decaying in the standard way into $f\bar{f}$. For very low Higgs masses, it is predicted to decay into $\gamma\gamma$ or into e^+e^- with a lifetime long enough to escape detection. This lifetime decreases rapidly when the mass

increases, so that if the mass is above 20 to 30 MeV/c^2, the decay products are within the detector. The invisible particle is searched through missing momentum in events in which the Z^{0*} decays in e^+e^- or $\mu^+\mu^-$. Above a few tens MeV/c^2, the main H^0 decay channel is e^+e^- and one searches for an isolated V^0 . All $f\bar{f}$ final states are used in this case. The results of this study are shown on figure 12 from the Opal experiment[26]: the combined result of these two searches clearly eliminates the possibility of a standard Higgs boson with a mass up to the $\mu^+\mu^-$ threshold.

At higher mass, the Higgs is predicted to decay mostly to the highest mass $f\bar{f}$ channel open. A complete study of these hadronic decays has been made at LEP, and the highest mass results from Aleph [27] are shown on figure 13: no mass below 41.6 GeV/c^2 is alllowed, so that the Higgs is not present in the com_ ι mass range [0-41.6]GeV/c^2 . Clearly, this search will be continued.

Other more complicated Higgs sectors are also studied, notably the two Higgs doublet models, which need 3 neutral and 2 charged particles. The charged Higgs are excluded below 42 GeV/c^2 , and the lightest neutral, called h^0, is excluded below 32 GeV/c^2 , independently of the mixing parameter between the doublets.

Conclusions

For its first year of operation, the LEP e^+e^- collider has already produced very fundamental results.

The Z^0 mass is now known to 3 10^{-4}, and is one of the precise input constants of the Standard Model

The number of neutrinos is 2.89 $\pm$ 0.10, and this constrains many cosmological models.

The effective value of $\sin^2\overline{\theta_W}$ at $M_Z{}^2$ is 0.2296$\pm$0.0020.

The top quark mass is below 200 GeV/c^2 .

The standard Higgs boson mass is not in the range 0 to 41.6 GeV/c^2 .

The minimal version of the Standard Model has been tested at unprecedented energies and precisions, and its validity remains up to now unchallenged, but much more precise measurements are still necessary to validate many of its aspects.

This could not have been possible without the splendid effort of the accelerator physicists and engineers who built LEP. It is timely to recall that the first time the mere possibility of this machine came to light was through the far-sighted work of B.Richter [28].

References

[1] F.Dydak, invited report to the XXVth Int. Conf. on High Energy Physics,Singapore, August 1990.

[2] B.Dehning, M.Placidi et al., to be published.

[3] Polarization at LEP, Report CERN 88-06, Geneva, 1988.

[4] F.A.Berends and R.Kleiss, Nucl. Phys. B228 (1983) 537;
M.Böhm, A.Denner and W.Hollik, Nucl. Phys. B304 (1988) 687;
F.A.Berends, R.Kleiss, and W.Hollik, Nucl. Phys. B304 (1988) 712.

[5] ALEPH Collaboration, D.Decamp et al., Phys. Lett. B235 (1990) 399, and Preprint CERN-PPE/90-104.

[6] DELPHI Collaboration, P.Abreu et al., Phys. Lett. B241 (1990) 435.

[7] L3 Collaboration, B.Adeva et al., Phys. Lett. B249 (1990) 341.

[8] OPAL Collaboration, M.Z.Akrawy et al., Phys. Lett. B240 (1990) 497.

[9] D.Bardin et al., in Z-Physics at LEP 1, Report CERN 89-08, pp 89sq, Geneva, 1989.

[10] M.Consoli et al., in Z-Physics at LEP 1, Report CERN 89-08, pp 7sq, Geneva, 1989.

[11] OPAL Collaboration, M.Z.Akrawy et al., Phys. Lett. B247 (1990) 458.

[12] L3 Collaboration, B.Adeva et al., preprint L3 #017, August 1990.

[13] DELPHI Collaboration, P.Abreu et al., preprint CERN-PPE/90-119.

[14] M.Böhm et al., in Z-Physics at LEP 1, Report CERN 89-08, pp 203sq, Geneva, 1989.

[15] ALEPH Collaboration, D.Decamp et al., preprint CERN-PPE/90-104.

[16] G.Goggi, in report CERN 79-01, p 483sq , Geneva, 1979.

[17] J.-E.Augustin, in report CERN 79-01, p 499sq , Geneva, 1979.

[18] P.Vaz, Measurement of $\tau^+\tau^-$ pairs from Z^0 decays, Thesis (1990), unpublished.

[19] J.C.Brient, XXVth Int. Conf. on High Energy Physics,Singapore, August 1990;
F.Zomer, Workshop on Tau Lepton Physics, Orsay, September 1990.

[20] UA2 collaboration, J.Alitti et al. Phys. Lett. B241 (1990) 150;
CDF Collaboration, P.Shalbach in Proceedings of the APS Washington Conference, April 1990.

[21] J.Ellis and G.L.Fogli, Phys. Lett. B249 (1990) 543.

[22] OPAL Collaboration, M.Z.Akrawy et al., Zeit. Phys. C47 (1990) 505.

[23] G.Kramer and B.Lampe, Fortschr. Phys. 37 (1989) 331.

[24] L3 Collaboration, B.Adeva et al., Phys. Lett. B248 (1989) 464.

[25] DELPHI Collaboration, P.Abreu et al., preprint CERN-PPE/90-122.

[26] OPAL Collaboration, M.Z.Akrawy et al., preprint CERN-PPE/90-116.

[27] ALEPH Collaboration, D.Decamp et al., Phys. Lett. B246 (1990) 306.

[28] B.Richter, Very High Energy Electron-Positron Colliding Beams for the Study of Weak Interactions, Nucl. Instr. & Meth. 136 (1976) 47.

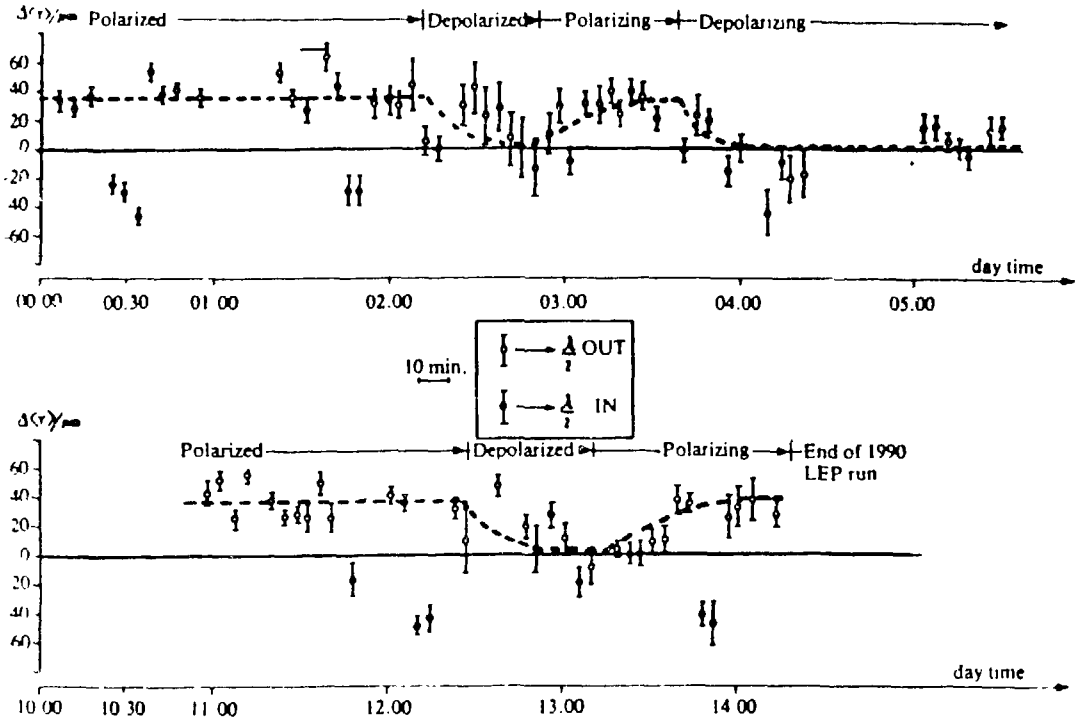

- Figure 1: Up-down asymmetry of polarized light backward scattered on the LEP beam. The solid points were measured with reverse circular polarization of the light (half wave length plate in).

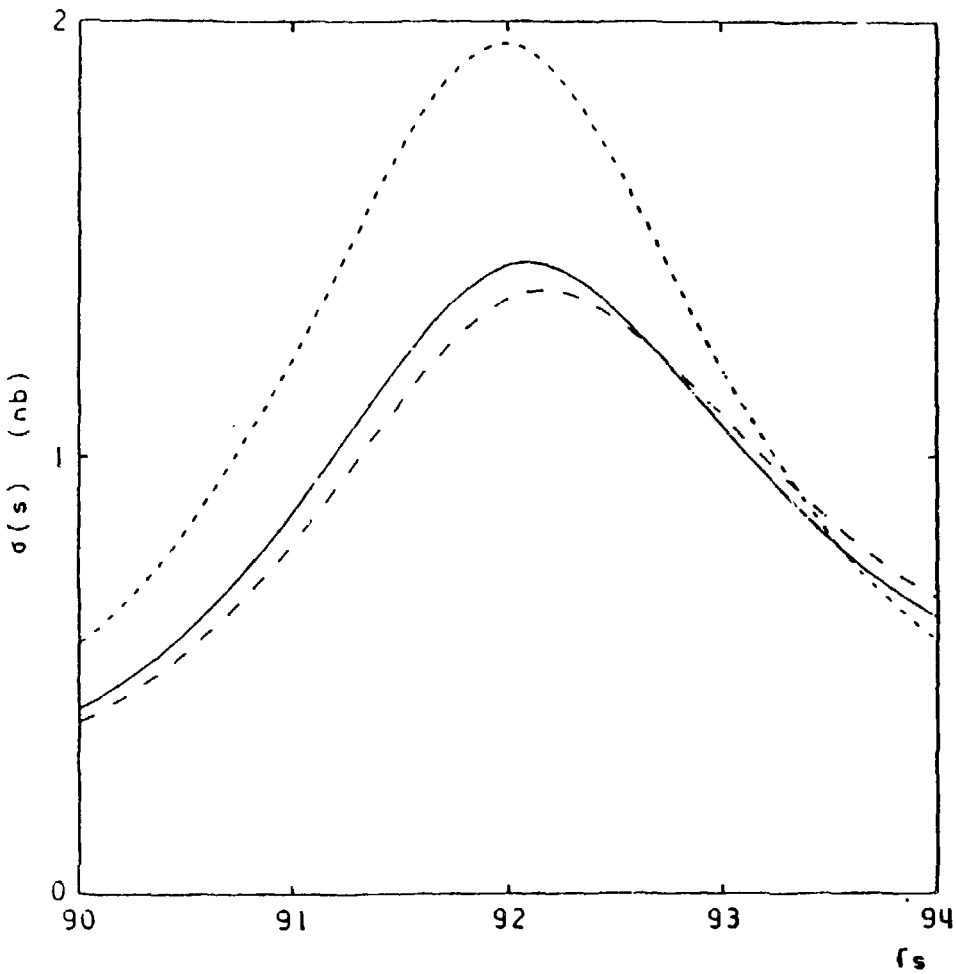

• Figure 2: Computed line-shape curves: uncorrected (fine dashed line), first order QED corrected (dashed line),and with second order corrections (solid line).

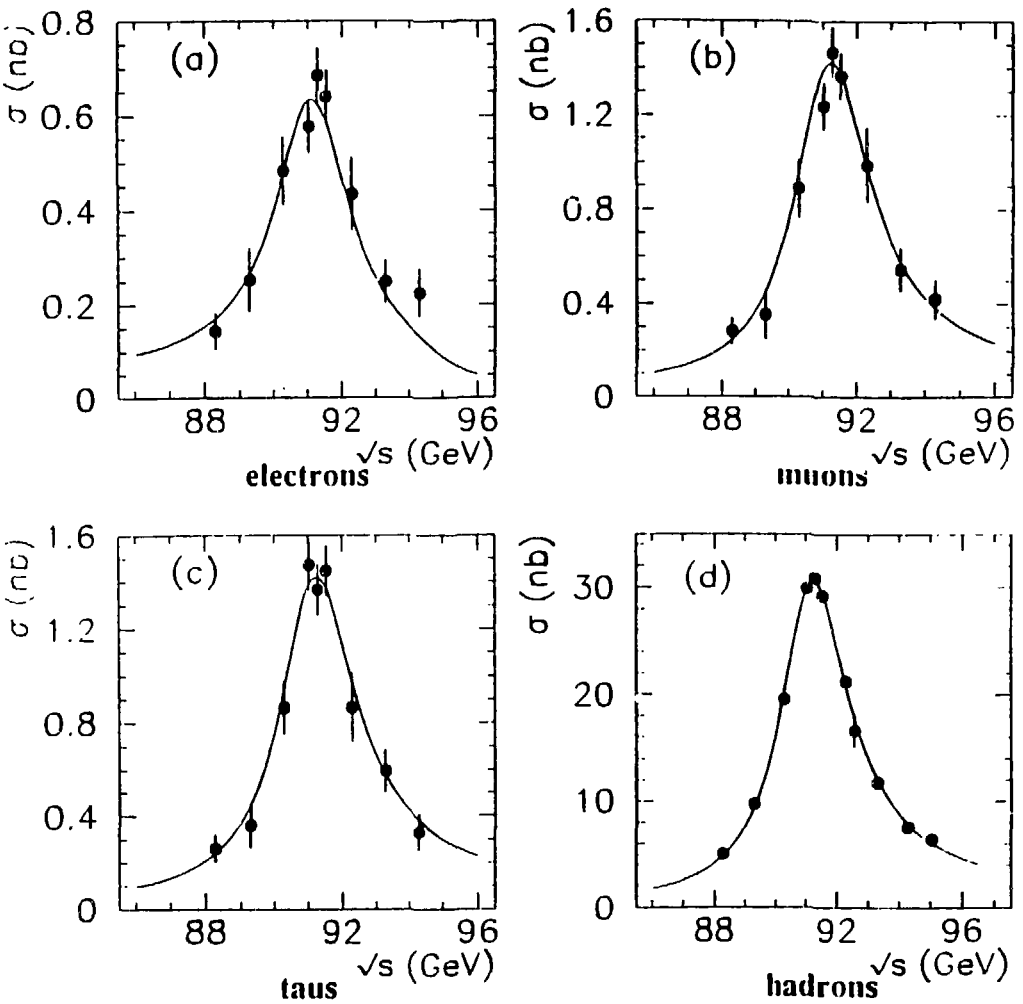

- Figure 3: Z^0 excitation curves observed[11] from electrons (a), muons (b), taus (c), and multihadrons (d).

(a)

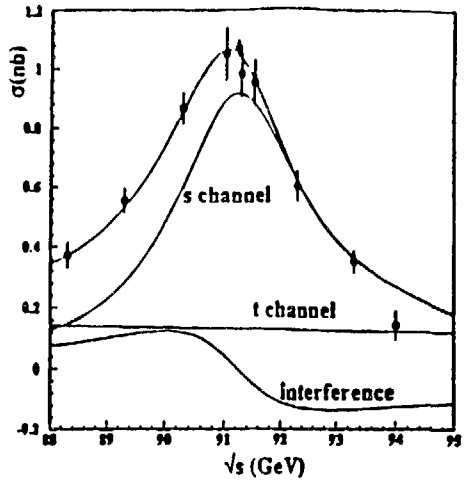

(b)

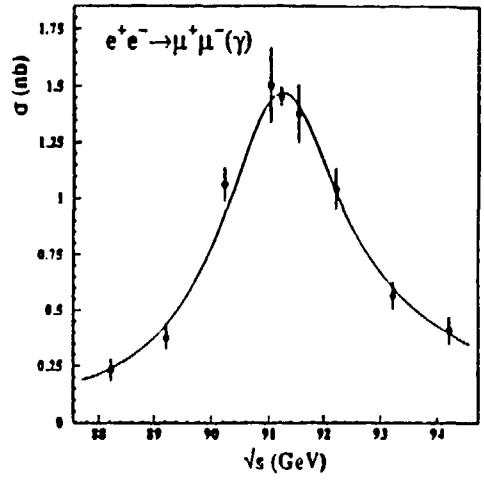

(c)

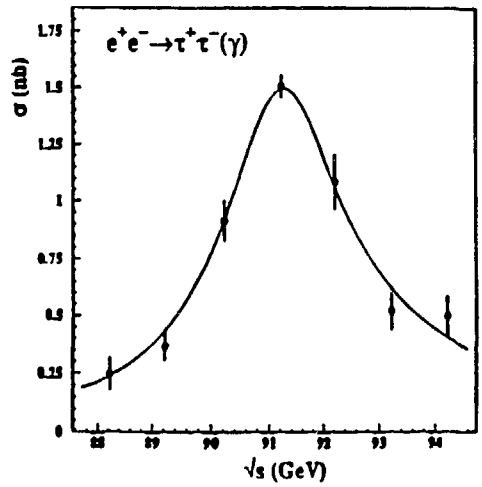

- Figure 4: e^+e^- cross-section measured[12] at large angles, compared with the s- and t-channel predictions(a). $\mu^+\mu^-$ (b) and $\tau^+\tau^-$ (c) measured cross-sections.

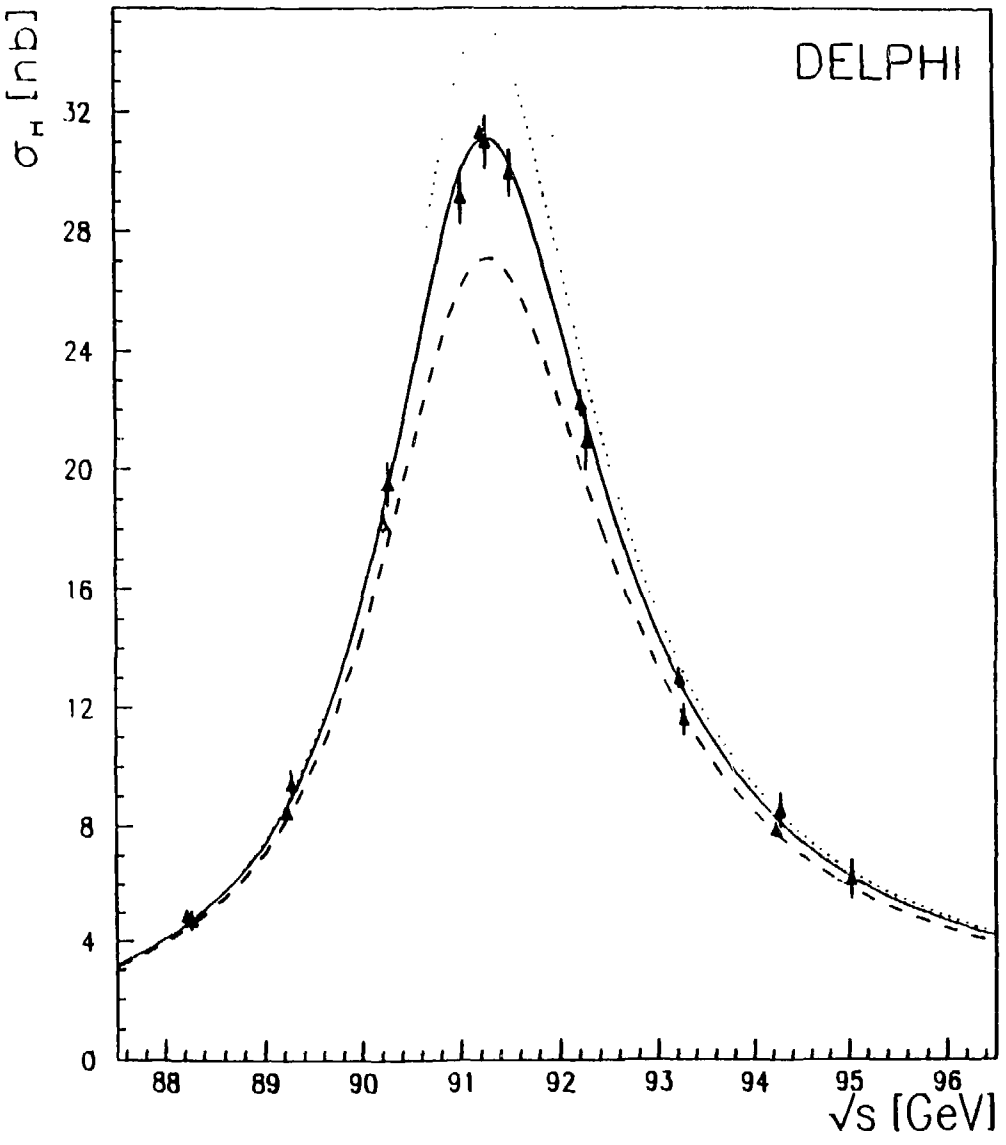

- Figure 5: Hadron excitation curve fit (solid line)[13], compared with predictions for $N_\nu = 2$ (dots) and $N_\nu = 4$ (dashed line).

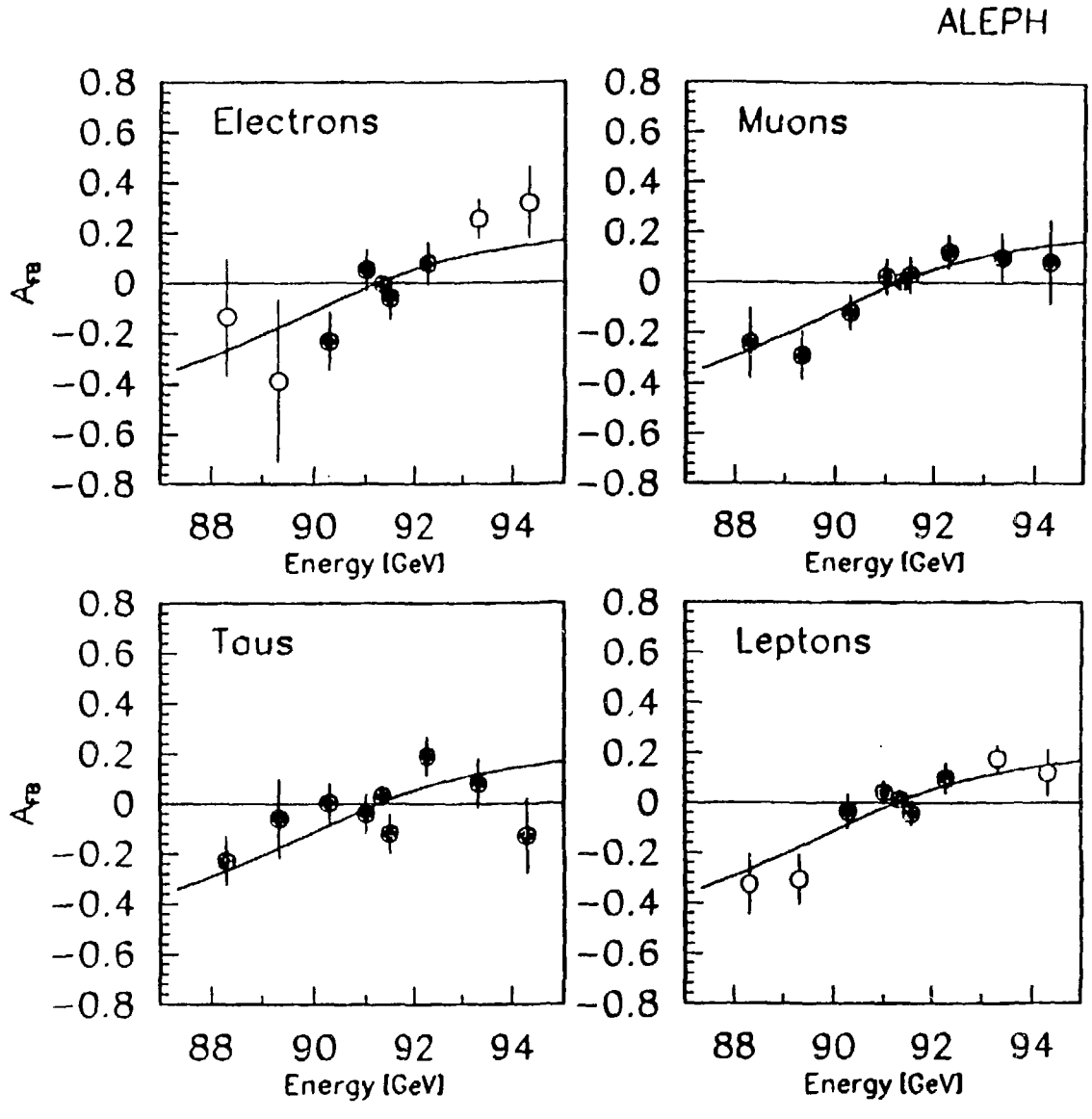

- Figure 6: Forward-backward asymmetry[15] for e^-, μ^-, τ^-, and for unseparated leptons, as a function of the center-of-mass energy.

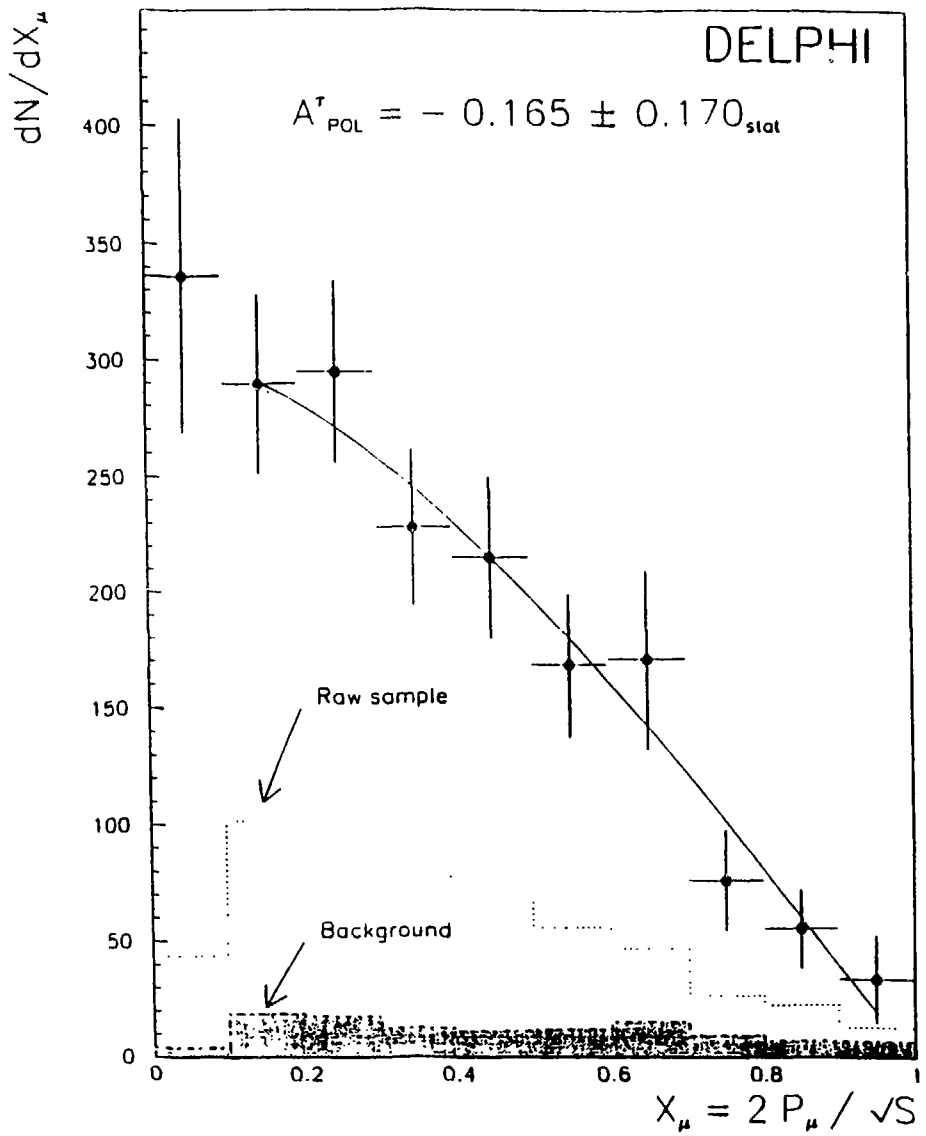

- Figure 7: Momentum spectrum of the μ emitted in the τ decay[18].

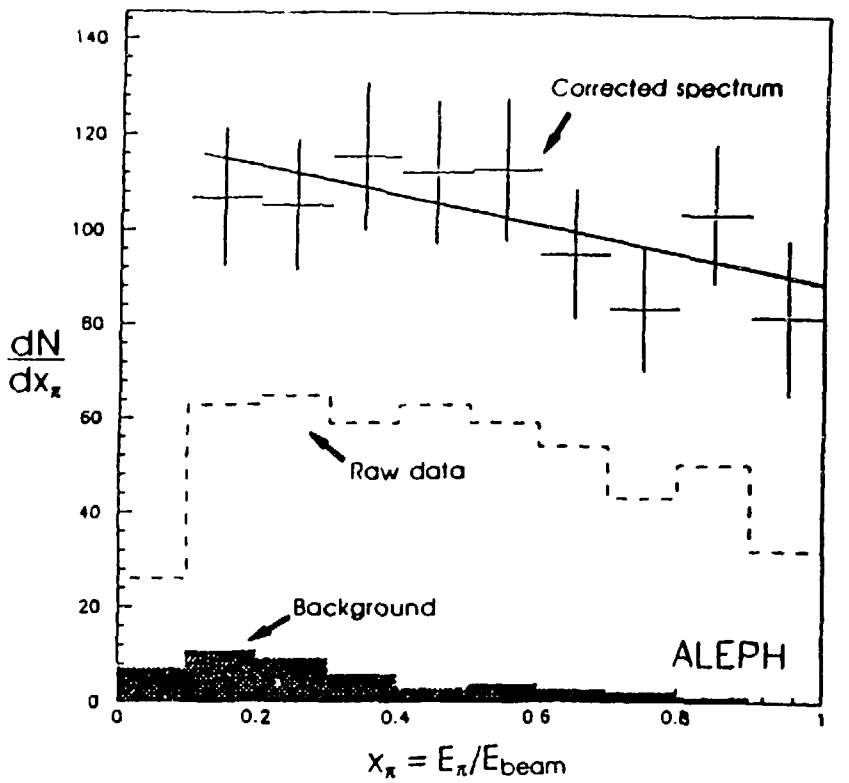

• Figure 8: Momentum spectrum of the π emitted in the $\tau \rightarrow \pi\nu$ decay[19]. The slope measures the polarization.

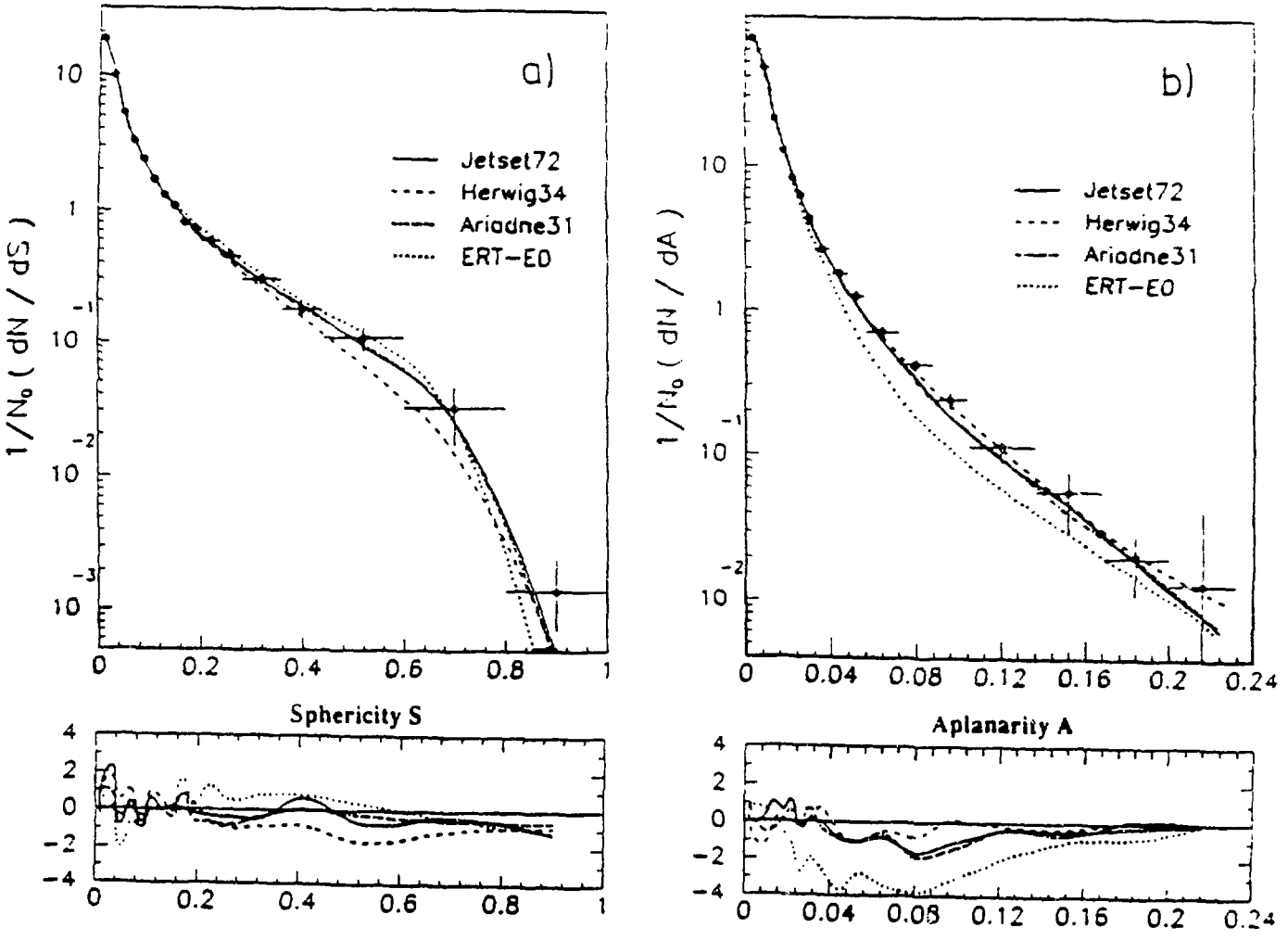

• Figure 9: Sphericity and aplanarity distributions[22] compared to predictions of optimized QCD models.

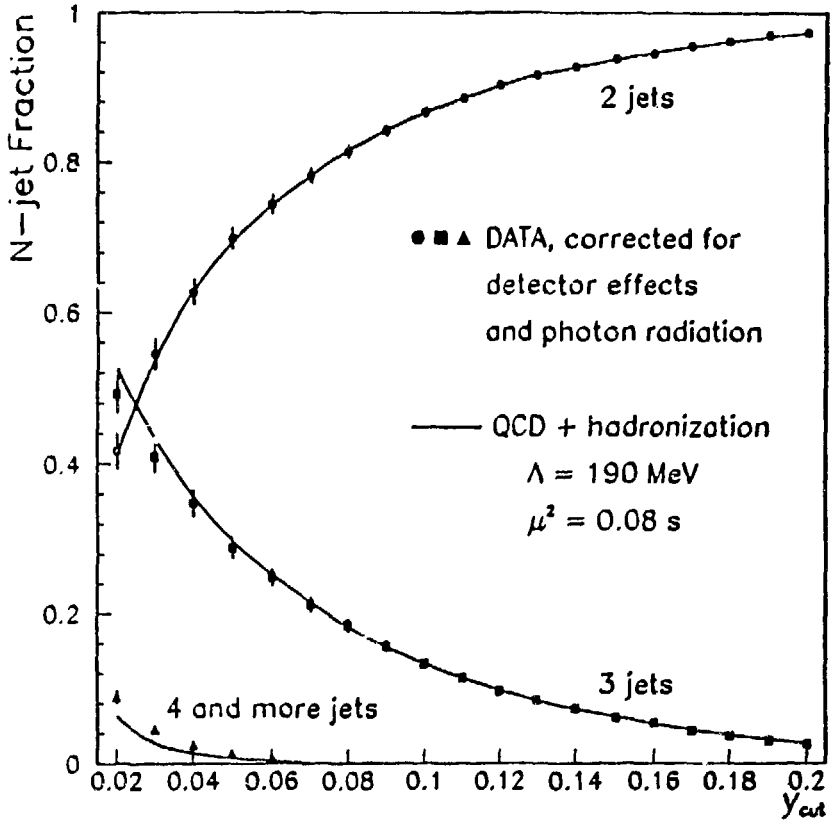

- Figure 10: Comparison of corrected measured[24] jet fractions and predicted jets rates in second order QCD.

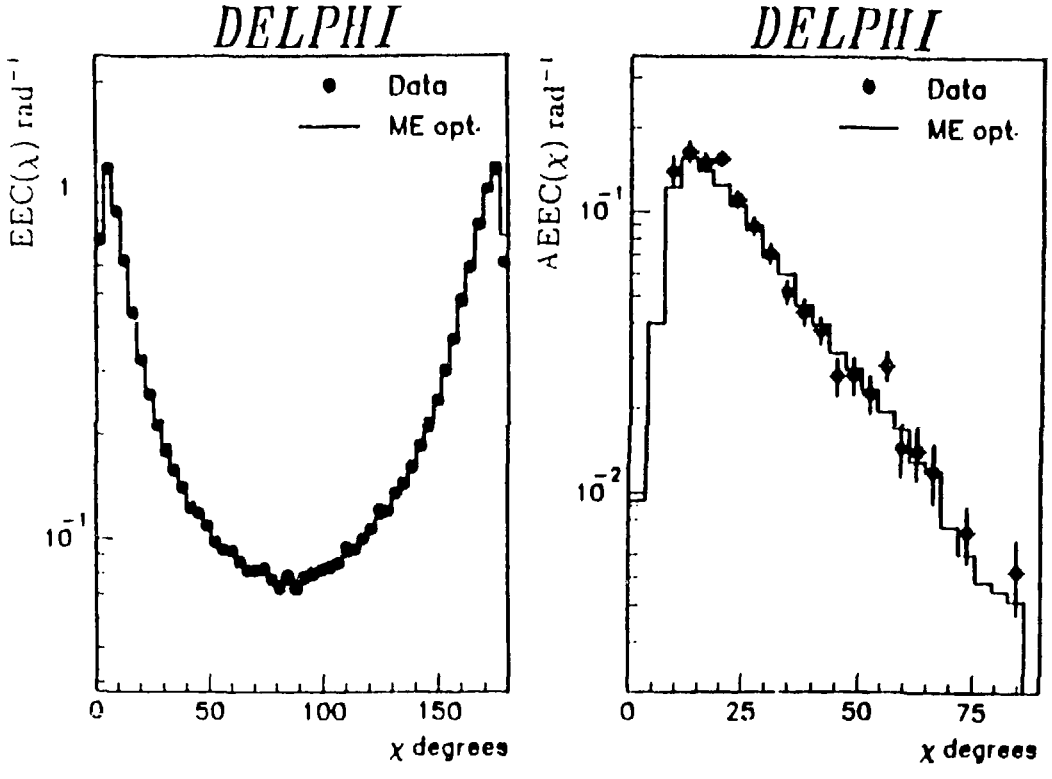

- Figure 11: Corrected energy-energy correlation distribution EEC, and corresponding asymmetry AEEC compared[25] with the Matrix Element Monte Carlo .

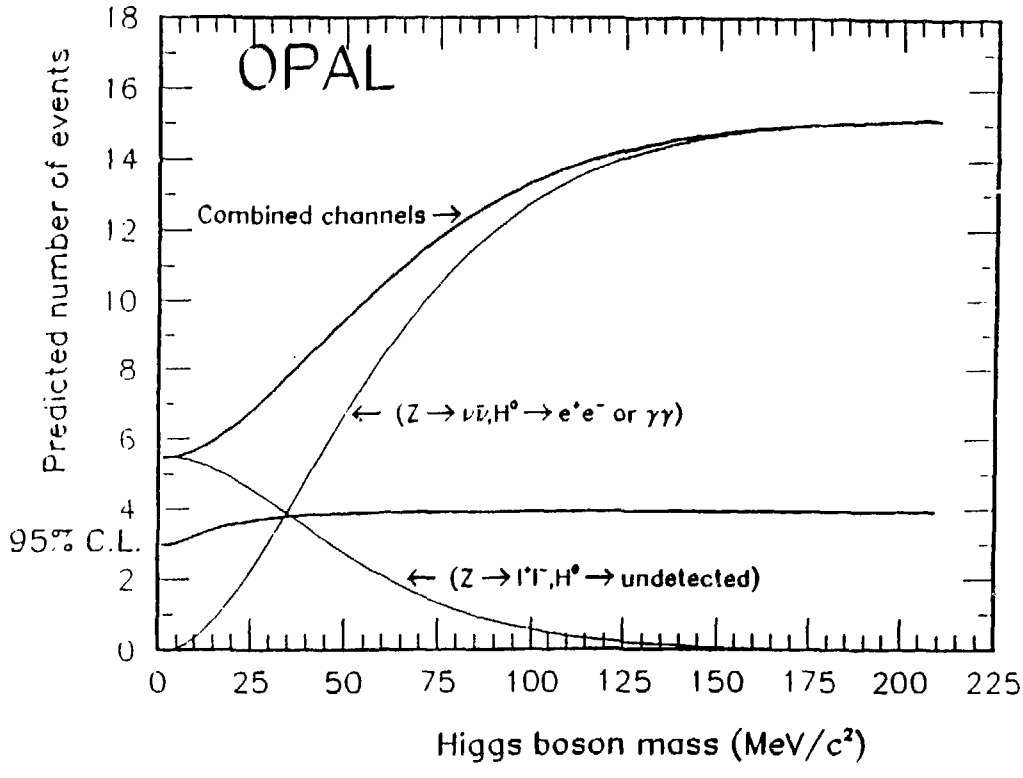

- Figure 12: Predicted number of detected H^0 vs. Higgs mass for very light Higgs boson masses[26].

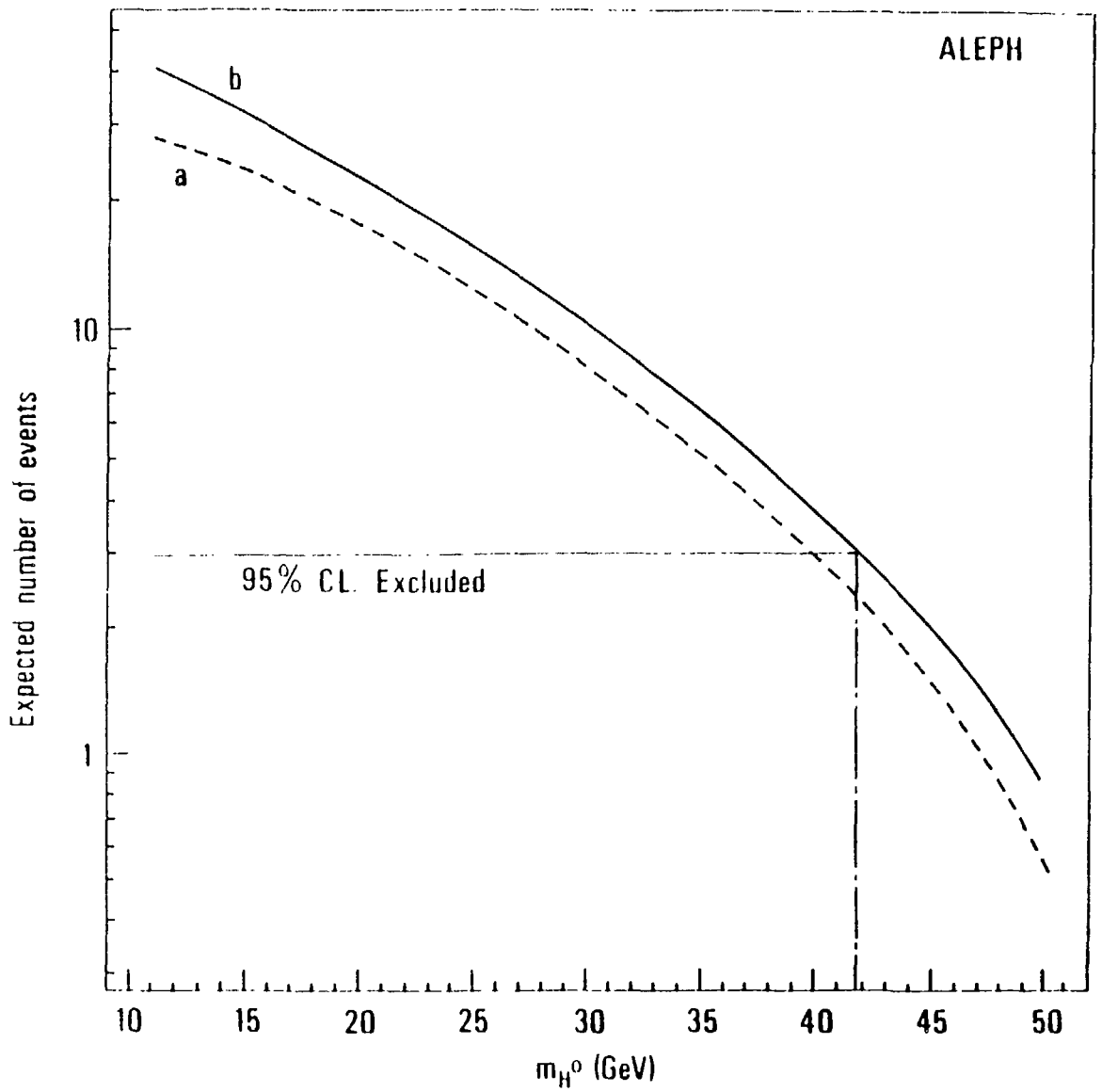

• Figure 13 Number of expected events from Z^0 decay into $H^0\nu\bar{\nu}$ (a) and into all channels (b) as a funtion of the Higgs mass[27].